Article

Modelling the effectiveness of an isolation strategy for managing mpox outbreaks with variable infectiousness profiles

Yong Dam Jeong [1,2], William S. Hart [1,3,15], Robin N. Thompson [3,15], Masahiro Ishikane[4,15], Takara Nishiyama[1], Hyeongki Park[1], Noriko Iwamoto[4], Ayana Sakurai[4], Michiyo Suzuki[4], Kazuyuki Aihara [5], Koichi Watashi [6], Eline Op de Coul [7], Norio Ohmagari [4], Jacco Wallinga [7,8], Shingo Iwami [1,5,9,10,11,12,13,16] ✉ & Fuminari Miura [7,14,16] ✉

The global outbreak of mpox in 2022 and subsequent sporadic outbreaks in 2023 highlighted the importance of nonpharmaceutical interventions such as case isolation. Individual variations in viral shedding dynamics may lead to either premature ending of isolation for infectious individuals, or unnecessarily prolonged isolation for those who are no longer infectious. Here, we developed a modeling framework to characterize heterogeneous mpox infectiousness profiles – specifically, when infected individuals cease to be infectious – based on viral load data. We examined the potential effectiveness of three different isolation rules: a symptom-based rule (the current guideline in many countries) and rules permitting individuals to stop isolating after either a fixed duration or following tests that indicate that they are no longer likely to be infectious. Our analysis suggests that the duration of viral shedding ranges from 23 to 50 days between individuals. The risk of infected individuals ending isolation too early was estimated to be 8.8% (95% CI: 6.7–10.5) after symptom clearance and 5.4% (95% CI: 4.1–6.7) after 3 weeks of isolation. While these results suggest that the current standard practice for ending isolation is effective, we found that unnecessary isolation following the infectious period could be reduced by adopting a testing-based rule.

Since May 2022, a global outbreak of mpox (formerly monkeypox) has spread primarily among men who have sex with men (MSM), first in European and North American countries, and later in other regions[1]. Although growth of the outbreak was initially rapid, the global trend in reported cases changed around the summer of 2022 and has been declining ever since[2]. Recent studies have suggested that the case saturation in many countries may be explained largely by infection-derived immunity accumulated among individuals who have many sexual partners[3], and the following decline in cases may have been accelerated by vaccination campaigns and/or behavioral changes[4,5]. However, since the beginning of 2023, sporadic outbreaks have been reported, mainly in Asian countries, which were less affected by the 2022 outbreak and where vaccination campaigns had not yet been initiated, leading to a substantial number of individuals remaining at risk of infection[6]. There are also reports of some breakthrough infections and reinfections in European countries[7,8]. These findings warrant caution against a resurgence of mpox and highlight the importance of maintaining nonpharmaceutical interventions (NPIs).

One essential NPI is case isolation. The effectiveness of isolation has been extensively studied in the context of COVID-19[9,10] and other diseases[11,12]. In general, if cases are detected earlier (e.g., via contact

tracing) and isolation begins sooner, a larger proportion of onward transmissions can be prevented[13]. When determining the end of isolation, later is always safer, as a longer isolation period minimizes the risk of exposure by individuals who remain infectious. However, case identification may require a substantial public health investigation effort, and redundant isolation induces societal cost and burden for individuals[14,15]. Furthermore, more stringent control strategies may also lead to reduced efficacy due to non-adherence[16]. To mitigate these burdens, testing-based rules were applied during the COVID-19 pandemic[17–19], which typically involved ending isolation following a specified number of successive negative PCR or antigen test results. Individual-level viral load data have been used to balance the effectiveness and cost of isolation rules[20], which is key to sustainable implementation.

The duration of the infectious period for mpox has yet to be quantitatively characterized. Several studies have investigated serial intervals (i.e., the time interval between symptom onset dates of primary and secondary cases in transmission pairs) as a proxy, and have suggested that more than 90% of transmission occurs within two weeks of symptom onset[21,22]. However, factors such as self-reporting may induce biases in serial interval estimates, and moreover, the serial interval distribution may be different to that of the infectious period. Recent findings have also indicated that there might be considerable heterogeneity in the infectious period among individuals with mpox; for example, there is substantial variation in observed serial intervals[21], and some confirmed cases in Europe have exhibited prolonged viral shedding in their bodily fluids[23,24]. Consequently, isolation rules that do not account for heterogeneity between individuals (e.g. rules based on isolating for a fixed period following symptom onset) may lead to either a risk of ending isolation too early for those who are infectious for long periods, or an unnecessarily long isolation period for those who are only infectious for short periods.

Current guidelines for mpox generally suggest quarantine of individuals exposed to mpox virus for about 3 weeks[18,25]. The three-week monitoring period is based on the estimated incubation period[18,25], in which more than 98% of people with mpox show symptoms within 21 days of exposure, to check if the exposed individual becomes symptomatic. However, the incubation period does not reflect the generation time of the virus, with onward transmission often occurring after symptom onset. Consequently, individuals whose symptoms have developed are recommended to isolate until their skin lesions have resolved (typically 2–4 weeks)[18,19,25–28] and are advised to refrain from sexual contact for 12 weeks after the end of isolation[25,27,28]. It should be noted that judging the clearance of symptoms for mpox is often difficult and quite subjective, as mild lesions can be undetected even at clinics[29,30]. This may result in misleading evaluations of individuals' risk of further onward transmission.

In this study, we first characterize individual infectiousness profiles among mpox cases by analyzing longitudinal viral load data. We describe the time course of virus shedding using a mathematical model that captures individual heterogeneity in the duration of viral clearance. We then stratify the population according to the characterized shedding profiles and evaluate the effectiveness of three different isolation rule types: a symptom-based rule (i.e., the typical current approach), a fixed-duration rule (i.e., a one-size-fits-all approach), and a testing-based rule (i.e., a personalized approach in which individuals end their isolation upon test results suggesting the individual is no longer infectious). Our study provides an approach to quantify both the risk of ending isolation too early and the period for which infected individuals are isolated but do not pose an infection risk. Our model can be used by policy makers to inform decision-making, allowing isolation strategies to be determined that balance cost and effectiveness appropriately.
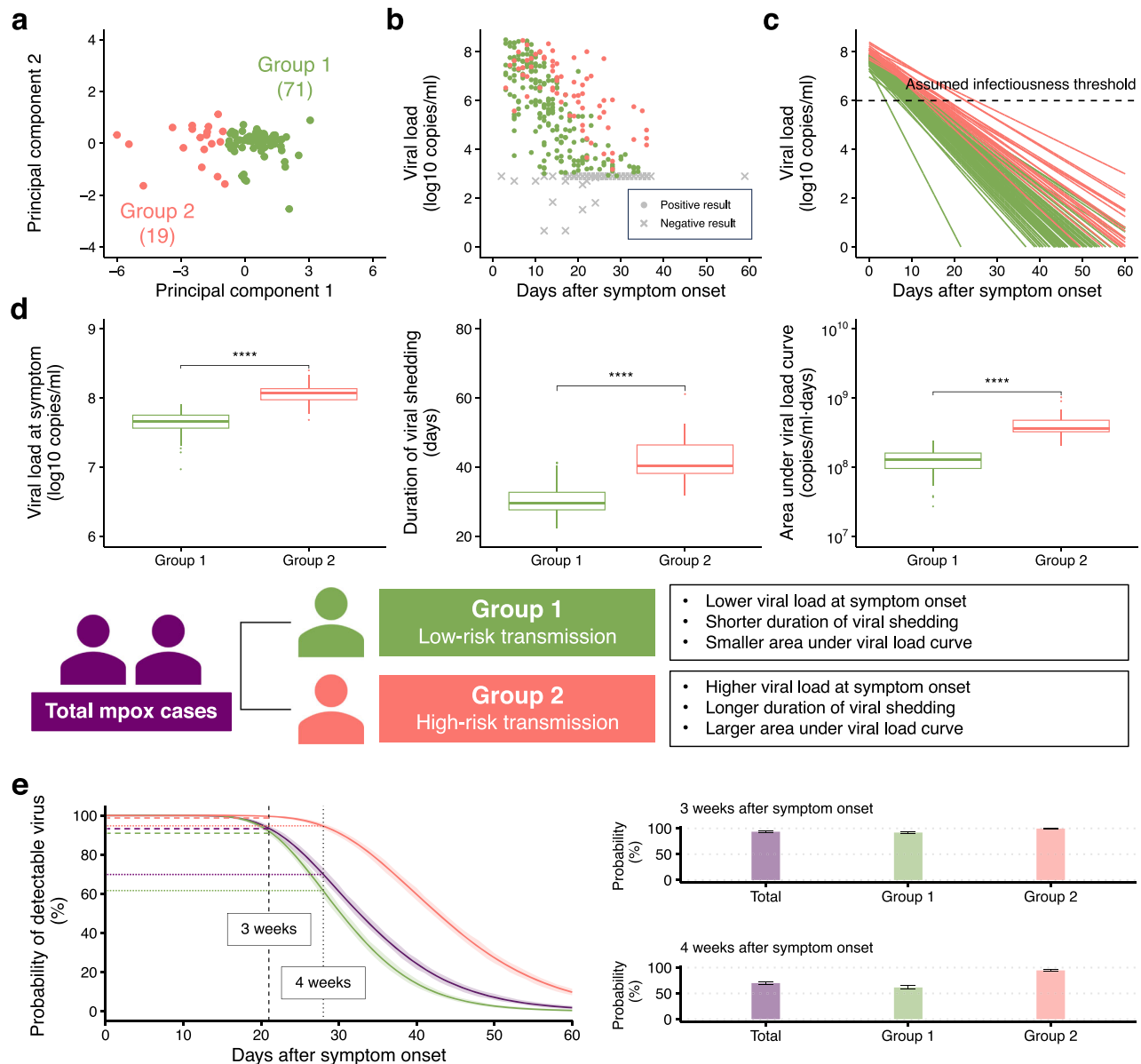
Results

Analyzed data and model fitting

We identified 7 publications including at least one case with lesion samples meeting the inclusion criteria, and a total of 90 mpox cases (see section "Methods"). All cases were symptomatic, and most of them were reported in Europe. To standardize the collected data, we converted the reported cycle threshold values to viral load (copies/ml) using the conversion formula proposed in a previous study[31] (Supplementary Table 1). We then fitted a viral clearance model to the longitudinal viral load data from lesion samples (Supplementary Fig. 1a and Supplementary Fig. 2). Estimated parameters suggested a median viral load of 7.7 log10 copies/ml (95% CI: 7.3–8.2) at symptom onset and a median viral clearance rate of 0.36 day^{-1} (95% CI: 0.24–0.44), respectively. Using these parameters, duration of infectiousness was estimated: we first assumed a threshold value for infectiousness as 6.0 log10 copies/ml based on data on viral replication in cell culture[23,32,33], and the duration of infectiousness was estimated to be 10.9 days (95% CI: 7.3–21.6) following the onset of symptoms. Additionally, a prolonged duration of viral shedding was estimated: the viral load dropped below the limit of detection of a PCR test (2.9 log10 copies/ml) 30.9 days (95% CI: 23.4–50.6) after symptom onset (Supplementary Fig. 1b). This finding is consistent with previous studies suggesting the persistent presence of mpox viruses in clinical specimens[23,34].

Stratification for mpox cases

The 90 analyzed mpox cases were stratified into two groups Group 1 and Group 2 (Fig. 1a–c), using the K-means clustering algorithm based on three estimated individual-level parameters: the viral load at symptom onset, the total amount of virus excreted between symptom onset and the end of shedding, and the duration of viral shedding (see Supplementary Note 2). Group 1 had a lower viral load at symptom onset and faster viral clearance, whereas Group 2 showed a higher viral load at symptom onset and slower viral clearance. As a result, the estimated duration of infectiousness in Group 2 was longer than in Group 1 (Fig. 1c and Supplementary Fig. 1b). To compare the viral dynamics between the two groups, we conducted statistical tests: Individuals in Group 2 had significantly higher viral loads at symptom onset than individuals in Group 1 ($p = 5.7 \times 10^{-10}$ from the Mann–Whitney test). Viral clearance was significantly slower in Group 2 than in Group 1 ($p = 2.1 \times 10^{-9}$ from the Mann–Whitney test). Also, individuals in Group 2 had a larger area under the viral load curve (AUC) ($p = 4.6 \times 10^{-11}$ from the Mann–Whitney test). Thus, Groups 1 and 2 were characterized as groups with low and high transmission potential, respectively (Fig. 1d). To describe the difference in timing of viral clearance, we also reconstructed the probability of virus being detectable over time by using the model with estimated parameters for each group (Fig. 1e). In both stratified groups, the probability was greater than 90% at 3 weeks after symptom onset. However, in the total group (i.e., a group of all analyzed cases), the probability dropped to 69.9% (95% CI: 67.0–73.2) at 4 weeks after symptom onset, which is the upper bound of the isolation period recommended by the CDC and ECDC[19,25]. The probability in Group 1 at 4 weeks after symptom onset was 61.6% (95% CI: 58.2–64.8), whereas the corresponding probability in Group 2 was 94.6% (95% CI: 93.1–96.0).

Symptom-based rule

Under the estimated viral dynamics, we compared three types of rules for ending the isolation of individuals with mpox: a symptom-based rule, a fixed-duration rule, and a testing-based rule. To assess the effectiveness of the three rules, we considered three metrics: (1) the risk of prematurely ending isolation, (2) the average estimated infectious period after ending isolation (where this period was defined to be zero for individuals who are no longer infectious at the time of ending isolation), and (3) the average estimated duration for which individuals were isolated unnecessarily after the end of their infectious period

Fig. 1 | Stratification of mpox virus infections. a Results of K-means clustering of mpox cases based on viral load at symptom onset, area under the viral load curve (AUC), i.e., the total amount of virus shed over time, and duration of viral shedding using estimated individual parameters. Data points indicate individuals and are colored based on the group that each individual is in. Principal component analysis (PCA) was used to visualize the clusters in two dimensions. Groups 1 and 2 comprise 71 and 19 mpox cases, respectively. **b** Stratified viral load data points measured in lesion samples. The cross represents data points where the viral load was below the limit of detection. **c** Reconstructed individual viral load trajectories in each group. The horizontal dashed line means the assumed infectiousness threshold. **d** Comparison between groups of: viral load at symptom onset (left panel); duration of viral shedding (middle panel); and area under viral load curve (right panel), respectively. The box-and-whisker plots show the medians (50th percentile; bold lines), interquartile ranges (25th and 75th percentiles; boxes), and 2.5th to 97.5th percentile ranges (whiskers). The sizes of Group 1 and Group 2 are 71 and 19 cases, respectively. Using the two-sided Mann–Whitney test, statistically significant differences between the two groups were found for viral load at symptom onset (p value $= 5.7 \times 10^{-10}$), duration of viral shedding (p value $= 2.1 \times 10^{-9}$), and area under viral load curve (p value $= 4.6 \times 10^{-11}$). Group 1 and Group 2 represent cases with low and high risk of transmission, respectively. **e** Viral clearance in each group. Probability of detectable virus after symptom onset for each group (left panel). The solid lines and shaded regions indicate means and 95% confidence intervals, respectively. The dashed lines and dotted lines stand for probabilities at 3 and 4 weeks after symptom onset, respectively. Bar plots represent the probabilities for 3 weeks (right upper panel) and 4 weeks (right lower panel) after symptom onset, respectively. The centers and error bars indicate means and 95% confidence intervals, respectively. Note that the estimated probabilities are based on 100 independent simulations.

(which could be positive or negative). Whether an individual was infectious or not was ascertained based on an assumed threshold viral load value (see section "Methods").

With these metrics, we first evaluated the current symptom-based isolation guideline (i.e., patients remain isolated until their skin lesions have cleared), accounting for variations in the timing of lesion clearance between individuals. We estimated distributions of the timing of lesion clearance using data from 43 mpox patients describing the duration of lesion presence (see section "Methods"). As a result, the mean duration from symptom onset to lesion clearance was estimated to be 25.2 days (95% CI: 21.6–29.7). The median and interquartile range (IQR) were 23.2 days and 17.6–30.7 days, respectively. The estimated values were consistent with typical current isolation periods of 2–4 weeks[18,19,25–28] (Supplementary Fig. 3 and Supplementary Table. 4).

In the total group, the risk of prematurely ending isolation was estimated to be 8.8% (95% CI: 6.7–10.5) and Group 1 had a lower risk of 4.9% (95% CI: 3.8–6.1). In addition, both stratified groups yielded an average estimated infectious period after ending isolation of lower than 1 day. However, in Group 2, the risk of prematurely ending isolation was 25.7% (95% CI: 23.8–28.0) with a longer estimated infectious period after ending isolation of 1.6 days (95% CI: 1.4–1.8). The mean estimated duration for which individuals in the total group were isolated unnecessarily after the end of their infectious period was 12.1 days (95% CI: 11.6–12.8), whereas Groups 1 and 2 had unnecessary isolation periods of 13.5 days (95% CI: 13.0–14.1) and 6.6 days (95% CI: 5.9–7.3), respectively (Supplementary Fig. 4).

Furthermore, to ensure isolation is ended safely, we considered an additional isolation period beyond the time of lesion clearance. To lower the risk of prematurely ending isolation below 5% and the estimated infectious period after ending isolation below 1 day, the total group and Group 2 required additional isolation periods of 3 and 10 days on average, respectively. However, no additional isolation periods were necessary for Group 1. The resulting unnecessarily prolonged isolation periods in the total group, Group 1, and Group 2 were estimated to be 15.1, 13.5, and 16.6 days on average, respectively (Fig. 2a).

In our main analyses, we assumed that the presence or absence of symptoms was independent of viral dynamics. However, as a sensitivity analysis, we evaluated the current symptom-based rule for the total group under different assumed relationships between individual viral dynamics and the duration of lesion presence (see section "Methods"). The risk of ending isolation prematurely was lower when increased and/or prolonged viral shedding was assumed to be more strongly correlated with slower lesion clearance—the estimated risk under our baseline assumption (i.e., that lesion clearance is independent of viral shedding) can therefore be considered as an upper bound. This is because, if the presence of lesions is shown to be positively correlated with viral shedding, patients with fast lesion clearance could end isolation safely, and thus the estimated risk under such conditions would be lower than the baseline assumption. The unnecessarily prolonged isolation periods in this supplementary analysis were found to be comparable to those under the baseline setting and were lower than 2 weeks on average (Supplementary Fig. 5).

Fixed-duration rule

Under a fixed-duration rule of ending isolation 3 weeks after symptom onset, the risk of ending isolation prematurely in the total group was estimated to be 5.4% (95% CI: 4.1–6.7). The average estimated duration for which individuals were isolated unnecessarily after the end of their infectious period was 8.3 days (95% CI: 8.0–8.6). Group 1 had a lower risk of ending isolation prematurely of 1.9% (95% CI: 1.0–2.9), and a longer unnecessary isolation period of 9.7 days (95% CI: 9.4–9.9). However, in Group 2, a higher risk of 25.7% (95% CI: 23.2–28.0) was estimated, with a shorter unnecessary isolation period of 2.8 days (95% CI: 2.4–3.1). To guarantee a risk of prematurely ending isolation below 5% and an estimated infectious period after ending isolation shorter than 1 day, we found that the total group, Group 1, and Group 2 needed to be isolated for 22, 19, and 29 days, respectively. In this case, the estimated duration for which individuals were isolated unnecessarily after the end of their infectious period was estimated to be 9.4, 7.7, and 10.8 days for the total group, Group 1, and Group 2, respectively (Fig. 2b).

Testing-based rule

For symptom-based and fixed-duration rules, isolation of individuals with mpox ends after lesion clearance or fixed-time period following symptom onset, so the three metrics considered here are determined by the mean symptom duration or the predefined isolation period (Fig. 2a, b). By contrast, a testing-based rule is dependent on both the time interval between tests and the exact criterion used for ending isolation (see section "Methods"). Under a criterion in which isolation ends following two consecutive PCR test results indicating loss of infectiousness with daily testing (similar to a criterion widely used for COVID-19)[17], the total group had a risk of prematurely ending isolation of 52.2% (95% CI: 49.7–54.6), and the estimated infectious period after ending isolation was calculated to be 2.3 days (95% CI: 2.1–2.5). Similarly, high risks of prematurely ending isolation, accompanied with an estimated infectious period after ending isolation longer than 1 day, were estimated in the stratified groups (first-row and second-row panels in Fig. 2c).

By varying the criteria (i.e., the required number of consecutive test results indicating loss of infectiousness and the time interval between tests), different testing-based isolation rules can be tested in terms of their effects on the three metrics. The risk of prematurely ending isolation and the estimated infectious period after ending isolation decreased with a longer interval between tests and with a larger number of consecutive test results indicating loss of infectiousness (first-row and second-row panels in Fig. 2c), whereas the estimated duration for which individuals were isolated unnecessarily after the end of their infectious period increased (third-row panels in Fig. 2c). Under the conditions that the risk of prematurely ending isolation is lower than 5% and the estimated infectious period after ending isolation is shorter than 1 day, the minimum value of the unnecessary isolation period in the total group was 7.4 days (95% CI: 7.1–7.7) with three consecutive test results indicating loss of infectiousness and an interval of 5 days between tests (purple triangles in Fig. 2c). Correspondingly, an isolation period of 20.1 days (95% CI: 19.7–20.5) was required on average. On the other hand, under the same conditions, stricter rules were needed for Group 2: four consecutive test results indicating loss of infectiousness and an interval of 2 days between tests were needed to minimize the estimated duration for which individuals were isolated unnecessarily after the end of their infectious period to 8.4 days (95% CI: 8.0–8.7), with a mean isolation period of 26.6 days (95% CI: 26.0–27.0) (red triangles in Fig. 2c).

To further evaluate the uncertainty in the test-based rule, we considered a different type of measurement error model (i.e., a proportional error model), where the error variance increases in proportional to the predicted mean viral load, and examined the corresponding difference in the total group as a sensitivity analysis (see section "Methods"). While the measurement error was constant in the main analysis (i.e., constant error model), the proportional error model described higher error variance near the assumed infectiousness threshold. As a result, a stricter optimal isolation rule was needed to lower the risk and the estimated infectious period after ending isolation below 5% and 1 day, respectively: four consecutive test results indicating loss of infectiousness and an interval of 3 days between tests. However, the minimized unnecessary period and corresponding optimal isolation period under the proportional error model were comparable to the constant error model (Supplementary Fig. 6).

Additionally, whereas we focused on PCR testing in our main analyses, we conducted further analyses considering rapid antigen tests (RATs) to evaluate the effectiveness of using different test types when applying the testing-based rule. Under the testing-based rules using RATs, test results correspond to negative results (i.e., measured viral loads below a limit of detection) (see section "Methods"). When RATs with either high or low sensitivity were utilized in the testing-based rule, the optimal isolation periods on average were comparable with those under PCR testing. However, the optimal testing rules for ending isolation differed depending on RAT sensitivity: 2 consecutive negative results with 3-day intervals between tests were optimal for the high sensitivity RAT and 5 consecutive negative results with 3-day intervals between tests were optimal for the low sensitivity RAT. In both scenarios, a higher number of total tests was required to meet the specified conditions (i.e., the risk of prematurely ending isolation ≤5%
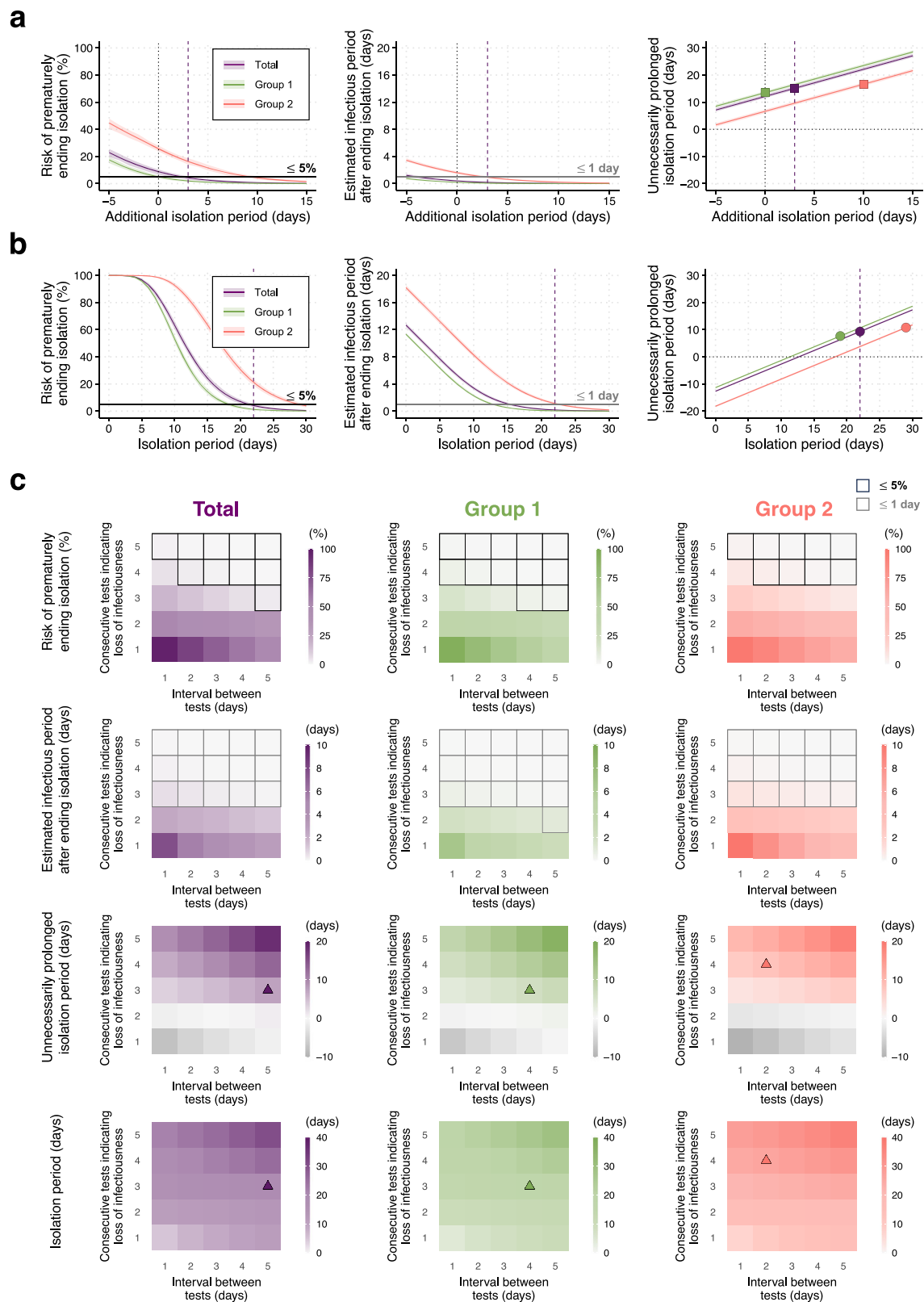
and the estimated infectious period after ending isolation ≤1 day) (Supplementary Fig. 7) than for PCR testing, since even high sensitivity RATs are typically much less sensitive than PCR tests (see Supplementary Note 5 and Supplementary Fig. 8). Additionally, RATs only provide qualitative test results (i.e. positive or negative), making it impossible to determine whether an individual who tests positive has a viral load that has fallen below the assumed infectiousness threshold.

Comparison between three different isolation rules for ending isolation

To highlight the difference between the three isolation rules for each group, we compared the three types of rule by computing the optimal rules in which the estimated isolation period following the end of infectiousness is minimized while ensuring that the risk of prematurely ending isolation is less than 5% and the estimated infectious period

Fig. 2 | Three different isolation rules for different groups. a Symptom-based rules. The vertical dotted lines mean the current symptom-based isolation guideline. The x-axis represents the additional isolation period from the current guideline. **b** Fixed-duration rules. The x-axis represents the fixed period of isolation. Left panels in both **a** and **b** show the risk of prematurely ending isolation for different isolation periods. The horizontal lines correspond to 5%. Estimated infectious period after ending isolation for different isolation periods (middle panels). The horizontal lines correspond to 1 day. The estimated period for which individuals are isolated unnecessarily after the end of their infectious period for different isolation periods (right panels). The squares and circles indicate the points with the lowest unnecessarily prolonged isolation period for which the following conditions are satisfied: i) the risk of prematurely ending isolation is lower than 5% and ii) the estimated infectious period after ending isolation is shorter than 1 day. The vertical dashed lines correspond to the optimal additional isolation period and the optimal fixed duration of isolation in the total group for symptom-based rules and fixed-duration rules, respectively. The solid lines and shaded regions in each panel indicate means and 95% confidence intervals, respectively. **c** Testing-based rules. The risk of prematurely ending isolation (first row of panels), the estimated infectious period after ending isolation (second row of panels), the estimated isolation period following the end of infectiousness (third row of panels), and the overall isolation period (fourth row of panels) are shown for different intervals between tests and numbers of consecutive tests indicating loss of infectiousness necessary to end isolation. PCR (polymerase chian reaction) tests (limit of detection = 2.9 log10 copies/ml) were used to measure viral load. The areas surrounded by solid lines are those with 5% or lower risk of prematurely ending isolation and with 1 day or shorter estimated infectious period after ending isolation, respectively. The triangles correspond to the points with the shortest estimated isolation period following the end of infectiousness for which both conditions noted above are satisfied. Color keys and symbols apply to all panels. Note that the estimated values are based on 100 independent simulations.
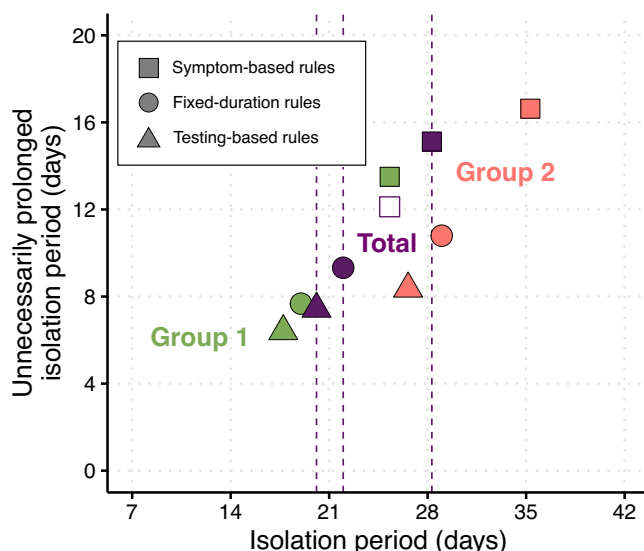
Fig. 3 | Comparison between three different isolation rules for different groups. The filled squares, circles, and triangles represent symptom-based, fixed-duration, and testing-based rules, respectively. Each symbol represents the mean length of isolation using the rule that minimizes unnecessarily prolonged isolation under the conditions that the risk of prematurely ending isolation is less than 5% and the estimated infectious period after ending isolation is less than 1 day. Note that for testing-based rules, the interval between tests and the number of consecutive tests indicating loss of infectiousness necessary to end isolation were chosen to minimize the unnecessarily prolonged isolation period. The vertical lines indicate the optimized isolation periods of three isolation rules for the total group. The unfilled square with outline indicates the current (non-optimized) symptom-based rule for the total group.

after ending isolation is less than 1 day (squares, circles, and triangles in Fig. 2). In the total group, the optimized symptom-based (i.e., current guideline +3 days), fixed-duration, and testing-based rules gave isolation periods of 28.3, 22, and 20.1 days, resulting in minimized unnecessary isolation periods of 15.1, 9.4, and 7.4 days on average, respectively (Fig. 3). In particular, compared to the current (non-optimized) symptom-based rule, the other two optimized rules involved shorter isolation periods and reduced unnecessarily prolonged isolation periods. In Group 2, the testing-based rule led to an unnecessary isolation period that was 8.2 and 2.4 days shorter than the symptom-based and fixed-duration rules, respectively. The testing-based rule in Group 1 yielded an unnecessary isolation period of 7.1 days shorter than the symptom-based rule, whereas it was comparable to the fixed-duration rule. However, compared with the other two rules in the total group, the testing-based rule in Group 1 could

reduce the unnecessary isolation period to 17.7 days, with the optimal isolation period of 6.4 days.

In addition, to assess the effectiveness of the testing-based rule, we examined the difference between the testing-based rule and the other two rules in the total group. The considered conditions for this assessment were; three consecutive test results indicating loss of infectiousness and a 5-day interval between tests for the testing-based rule (Fig. 2c), the current isolation guideline (i.e., the estimated duration of lesion presence) for the symptom-based rule, and the 22-day isolation period for the fixed-duration rule (Fig. 2a, b). Compared with symptom-based and fixed-duration rules, 63.2% (95% CI: 60.8–66.0) and 63.5% (95% CI: 60.6–65.4) of the total group could reduce their isolation periods using the testing-based rule, respectively (Supplementary Fig. 9a). The mean isolation period was shortened by 10.8 and 5.5 days compared to symptom-based and fixed-duration rules, respectively, and the average unnecessarily prolonged isolation period was also effectively reduced (Supplementary Fig. 9b, c). In these cases, the total number of tests required for ending isolation in the testing-based rule was estimated to be from 3 to 7 times (Supplementary Fig. 9d).

As a sensitivity analysis, we varied the assumed infectiousness threshold and investigated the corresponding difference in the estimated period for which individuals were isolated unnecessarily after the end of their infectious period between the three rules (Supplementary Fig. 10). When the assumed infectiousness threshold is higher, the corresponding estimated infectious period becomes shorter, leading to a shorter required isolation period and shorter period of unnecessary isolation given the same acceptable risk. Our analysis showed that a higher assumed infectiousness threshold resulted in smaller differences between the fixed-duration and testing-based rules for each stratified group, which was consistent with our previous findings for COVID-19[9]. On the other hand, simulations for the symptom-based rule in the total group suggested that the current guideline would lead to safer ending isolation but longer unnecessary isolation periods if the assumed infectiousness threshold value was increased.

We used an assumed infectiousness threshold of the viral load (6.0 log10 copies/ml) as a cut-off value for assessing isolation rules in the main analysis; however, other metrics for the risk of prematurely ending isolation could also be considered. To demonstrate this, we estimated the average area under the viral load curve (AUC) following the end of isolation for the total group under the different isolation rules, and compared the estimated values with the AUC without isolation (see Supplementary Note 6). Without any isolation, the average AUC was estimated to be $10^{8.5}$ copies/ml·days (95% CI: $10^{8.4}$–$10^{8.6}$). On the other hand, the estimates of average AUC after ending isolation were $10^{6.3}$ copies/ml·days (95% CI: $10^{6.1}$–$10^{6.5}$), $10^{6.0}$ copies/ml·days (95% CI: $10^{5.8}$–$10^{6.1}$), and $10^{5.8}$ copies/ml·days (95% CI: $10^{5.7}$–$10^{5.9}$) under the

current isolation guideline (i.e., the estimated duration of symptoms) for the symptom-based rule, the 22-day isolation period for the fixed-duration rule, and three consecutive test results indicating loss of infectiousness and a 5-day interval between tests for the testing-based rule, respectively. Compared to the case of no isolation, the average AUC was reduced by more than 95% under all three isolation rules, with the optimized testing-based rule giving the greatest reduction in the AUC (Supplementary Fig. 11). This indicates that the risk of prematurely ending isolation can be limited through those isolation rules.

Additionally, to highlight the necessity of the optimal isolation strategy (i.e., three consecutive test results indicating loss of infectiousness and a 5-day interval between tests) for the testing-based rules, we compared its average AUC to one under the other testing strategy. Since the mpox viral load continuously decreases over time since symptom onset, only one test result may be considered sufficient to guarantee the loss of infectiousness. However, this strategy may miss the ongoing infectiousness due to the measurement error (Supplementary Fig. 12a), whereas the optimal isolation strategy may end isolation more safely (Supplementary Fig. 12b). The average AUC under the strategy with one test result indicating loss of infectiousness and a 5-day interval between tests was estimated to be $10^{7.8}$ copies/ml·days (95% CI: $10^{7.7}-10^{7.9}$), much higher than one under the optimal testing strategy (Supplementary Fig. 12c).

As a sensitivity analysis, we considered an alternative two-phase exponential decay model[35], estimated the viral dynamics, and assessed the effectiveness of different isolation rules. In this additional analysis, to ensure that the parameters were identifiable, we used data from 30 cases (out of 90 cases with lesion samples) for which the viral load in lesion samples was recorded at four or more time points (see Supplementary Note 7). Compared to the baseline model (one-phase exponential decay model), the two-phase model indicated a higher viral load at symptom onset with a faster clearance in the first phase but with a slower clearance in the second phase (Supplementary Fig. 13a, Supplementary Fig. 14, and Supplementary Table 5), resulting in a longer estimated duration of infectiousness ($p = 2.1 \times 10^{-4}$ from the Mann-Whitney test) (Supplementary Fig. 13b). However, there was no significant difference in the duration of viral shedding between the baseline model and the two-phase exponential decay model (Supplementary Fig. 13c). For symptom-based and fixed-duration isolation rules under the two-phase exponential decay model, longer isolation periods on average were needed for ending isolation than using the baseline model. On the other hand, under the testing-based rules, the required isolation period was comparable with the baseline model (Supplementary Fig. 13d). Consequently, in the two-phase exponential decay model, the testing-based rules again substantially reduced the unnecessary duration of isolation, with shorter required isolation periods than under the symptom-based and fixed-duration rules.

Comparison between lesion and other samples for infectiousness after ending isolation

To demonstrate that lesion samples are suitable for designing isolation rules, we compared the viral dynamics that we inferred using lesion samples to analogous results obtained using other samples. Specifically, we used longitudinal viral load data measured in upper respiratory tract, blood, and semen samples from the same mpox cases to estimate mpox virus dynamics in those samples (Supplementary Table 1, Supplementary Table 2, Supplementary Fig. 15a, and Supplementary Fig. 16). Following symptom onset, other samples exhibited lower viral loads compared with lesion samples. For example, at the optimal ending isolation period of 22 days under fixed-duration rules, the viral load in lesion samples was substantially higher than in other samples (Supplementary Fig. 15b). Moreover, we compared the predicted infectiousness in lesion samples and other samples by estimating the proportion of individuals who remained infectious on day 22 after symptom onset. Around 3% of individuals were estimated to be infectious when lesion samples were used, whereas the viral load never exceeded the assumed infectiousness threshold for the other samples (Supplementary Fig. 15c). This suggests that infectious individuals with mpox may be missed if we implement a testing-based rule with samples other than lesion samples.

Discussion

In this study, we have compared the effectiveness of different rules that can be implemented to determine when individuals with mpox stop isolating. For the current symptom-based rule, our results showed that after skin lesions have disappeared, an additional 3-day isolation ensures the safe end of isolation. If instead a single population-wide fixed-duration rule is used, then we found that allowing individuals to end their isolation after a period of three weeks following symptom onset is a reasonable threshold. Under these rules, our transmission model suggests that more than 95% of post-diagnosis transmissions would be prevented. Our modelling analysis showed that there is individual heterogeneity in viral shedding kinetics, indicating that the use of testing-based rules may reduce the period for which infected individuals with a shorter duration of virus shedding are required to isolate.

Because we observed different shedding kinetics between mpox cases in the analyzed data, we stratified the cases based on their viral load during the decay phase of infection (Fig. 1). Variations in virus shedding may lead to substantial heterogeneity in infectiousness between individuals. For mpox, existing studies have focused on individual variations in the number of sexual contacts or partners[4,36], because higher contact rates generally result in a larger number of secondary cases. In contrast, variations in viral shedding have received limited attention to date. Our study found that about 32% of mpox cases exhibit a 5-10-day shorter (or longer) duration of virus shedding than the average. Such individuals may thus contribute to virus transmission for shorter (or longer) periods, resulting in a lower (or higher) number of secondary cases. When designing tailored interventions to ensure that the time-dependent reproduction number, R (the average number of secondary cases generated by each infected individual)[37], is below one (i.e., the outbreak is declining), our approach provides a way to incorporate such heterogeneity in the infectious period by using individual viral load as a proxy.

For evaluating the risk of transmission following the end of isolation, the use of longitudinal viral load data may be advantageous over symptom-based rules. One difficulty lies in the inherent uncertainty in self-reported symptoms; many confirmed mpox cases have been found to be not fully aware of their symptoms at the time of reporting[38]. Also, the precise identification of visible clearance of skin lesions poses a challenge in determining the end of isolation. Viral load data have the potential to provide more objective and quantitative criteria for ending isolation[39]. If viral load data are used, measuring viral load in lesion samples (rather than the other sample types that we considered) is the safest choice, as lesion samples showed the highest viral load and the longest detectable period (Supplementary Fig. 15).

Isolation rules need to balance the risk of exposure by individuals who remain infectious and the societal burden of extended isolation. Our results indicate that optimized symptom-based, fixed-duration, and testing-based rules can result in comparable risk levels if the same rule is applied to all cases. By contrast, the total duration of unnecessary isolation can be reduced using a testing-based rule. It is possible to shorten the isolation period for those with faster viral clearance, leading to a reduced burden at the population level. Furthermore, our simulation results showed that about 3−7 total tests were required by most individuals under the optimized testing-based rule (Supplementary Fig. 9). The estimated reduced isolation duration and testing frequency could be used to assess the cost-effectiveness of different strategies in future studies if additional information (e.g. the costs of prolonged isolation or PCR testing) can be obtained or estimated.

A testing-based rule may also be beneficial for evaluating the times at which individuals can resume sexual activities. Despite the current recommendation of using a condom for 12 weeks after scabs have fallen off as a precaution[25,27,28], having additional information about patients' infectiousness would offer reassurance to them and help to prevent discrimination and stigma related to sexual behaviors. As outlined in Supplementary Fig. 15, our assessment revealed that viral load in semen had fallen below the assumed infectiousness threshold by the endpoint of an optimized fixed-duration isolation period of 22 days. However, this result requires careful interpretation, since the threshold viral load above which transmission can occur is likely to depend on the precise route of transmission, in addition to other factors (e.g. scars on the skin).

As with any modelling analysis, there are limitations to our study. For example, our analysis relied on the patient data collected, which may not be representative of all mpox cases in the affected population. The estimated parameters were obtained using data from untreated patients, but in outbreak settings antiviral drugs such as tecovirimat may be provided to individuals with mpox and used prophylactically. Further investigations into the association between clinical characteristics of patients (e.g., medication history, smallpox vaccination status, and symptom severity) and viral load would be needed for a more granular understanding of heterogeneous infectiousness profiles. This may enable, for example, different isolation periods to be specified for individuals with different characteristics. Another limitation of this work is that the duration of lesion presence was estimated independently of the mpox viral load data. Since there were no available data to analyze the relationship between lesion clearance and mpox viral kinetics, we assumed these features to be independent in our main analysis. Accordingly, we conducted sensitivity analyses for the symptom-based rule by incorporating a dependency between the two features (Supplementary Fig. 5), demonstrating that our main estimates of the risk of premature release from isolation under the current rule may be upper bounds in practice.

Of course, the relationships between viral dynamics, symptoms and transmission are likely to be complex. For example, individuals would be more likely to refrain from sexual activities when lesions are still present, resulting in a lower risk of transmission. In addition, mpox virus shedding may not be exactly concurrent with the presence of symptoms, as has been demonstrated for other viral infections. For example, viral shedding of SARS-CoV-2 does not coincide with COVID-19 symptoms[40], and in genital herpes caused by HSV (Herpes Simplex Virus), viral elimination typically occurs when lesions are still present and visible[41]. The presence of lesions may not always be a good indicator of transmission risk, potentially leading to even more unnecessary isolation in some scenarios. If coupled viral load and lesion clearance data become available, the relationship between viral dynamics and symptoms could be analyzed more clearly; this is an essential target for future work. Similarly, the association between mpox viral load and infectiousness needs to be understood more deeply. Based on experimental data on viral culturability, we used 6.0 log10 copies/ml as an assumed threshold value for infectiousness in our main analysis; however, this estimate is uncertain[23,32,33]. We therefore performed sensitivity analyses (Supplementary Fig. 10) and found similar qualitative results about the relative effectiveness of different strategies regardless of the assumed threshold value. Also, since the in vitro-in vivo relationship on the culturability of mpox is not well understood, the assumed infectiousness threshold has not been validated in vivo for human sexual transmission. If coupling epidemiological data and viral load data at the individual level becomes available, we could estimate the infectiousness threshold in vivo in future studies. Furthermore, our analysis considered observation error in the testing-based rules but did not explicitly capture external sources of uncertainty that affect the false-negative rate of testing. In practical settings, imperfect swab sampling, especially with self-collection,

could occur (leading to different test specificity/sensitivity). There may also be who repeatedly test until they obtain a negative result, as occurred during the COVID-19 pandemic[42]. Such practical challenges need to be considered when implementing testing-based rules. Finally, our literature search was not completely systematic. The estimated viral dynamics may be biased towards those of patients who showed clear symptoms and were recorded in the collected datasets. Our analysis showed the substantial variability of viral dynamics across individuals; however, this result should be interpreted as the variation within the analyzed patient data, and there may be even larger individual variation if additional data of milder cases are incorporated.

In conclusion, despite the necessary simplifications of the modelling framework, this study provides empirical evidence for heterogeneity in virus shedding kinetics and infectiousness among mpox cases and describes the impact of such heterogeneity on the effectiveness of different isolation rules. Rules that recommend isolating until lesion clearance or following a fixed period after being exposed to the virus are straightforward to apply, and can be effective at preventing transmission. Rules that are instead based on obtaining test results indicating loss of infectiousness prior to ending isolation are more nuanced and can have advantages, for example by reducing the period for which some individuals are required to isolate after they are no longer infectious. Careful consideration of the benefits and drawbacks of different rules for ending isolation is essential. Ensuring sustainable implementation of NPIs remains key to responding effectively to future outbreaks of mpox and other diseases.

Methods
Study data
Longitudinal viral load data from mpox cases were obtained through literature searches using PubMed and Google Scholar. Specifically, the following query was used: ("Mpox" or "Monkeypox") and ("viral load" or "viral concentration" or "Ct value" or "cycle threshold") and ("skin lesion" or "lesion") and ("dynamics" or "kinetics" or "clinical course" or "symptom onset"). Further, we investigated articles from 2022 and 2023 identified in the search, reviewing each to extract the relevant data based on the following inclusion criteria: (1) time of symptom onset was recorded; (2) viral load was measured at least at two different time points (i.e., positive test results); (3) viral load was measured in different samples including lesion samples; and (4) patients did not receive any antivirals (as our model does not consider antiviral treatment). A total of 7 publications met those criteria, and 90 mpox cases were identified[23,24,29,43–46].

Additionally, we collected data on lesion clearance on mpox patients from the National Center for Global Health and Medicine (NCGM), Tokyo, Japan from July 2022 to November 2023. All mpox patients were diagnosed by polymerase chain reaction (PCR) for mpox using patient specimens. Data were collected on the following patient characteristics: date of birth, age, sex, race, clinical symptoms such as fever, skin lesion and annal pain, severe illness, treatment such as tecovirimat and vaccinia immune globulin intravenous. Severe illness was defined according to the mpox treatment guideline provided by the Disease Control and Prevention Center, National Center for Global Health and Medicine[47], and the Guidance for Tecovirimat Use by the Centers for Disease Control and Prevention of the United States of America[48].

Ethics declarations
For the longitudinal viral load data of mpox patients, we used only de-identified data from published studies and thus ethics approval was not required. For the lesion clearance data of mpox patients, this study was approved by the ethics committee of the National Center for Global Health and Medicine (NCGM) (approval no: NCGM-S-004748-00) and was implemented in accordance with the Declaration of Helsinki. Patient data were anonymized prior to the analysis. Due to the

retrospective nature of the study, the requirement of patient consent was waived.

Modelling mpox viral clearance and parameter estimation

Using the viral load data, we parameterized a mathematical model of temporal viral clearance dynamics in each infected individual. The collected viral load showed a decreasing trend over time since symptom onset (Supplementary Fig. 17), which was observed in other literature[23,49,50]. Thus, we employed an exponential decay model, which was previously utilized in a mpox study[23]:

$$\frac{dV(t)}{dt} = -\delta V(t), \tag{1}$$

where the variable $V(t)$ is the viral load (copies/ml) at time t and parameter δ represents the viral clearance rate. Note that the timescale is time after symptom onset; $t = 0$ is thus the date on which symptoms of mpox first began. $V(0)$ is the initial viral load at symptom onset.

A nonlinear mixed-effect model was used to estimate the parameters δ and $V(0)$[9,10]. This approach captures the heterogeneity in the viral dynamics by including both a fixed effect (the shared effect among individuals, i.e., population parameter) and a random effect (the individual-level effect) in each parameter. Population parameters and the standard deviation of random effects were estimated by using the Stochastic Approximation Expectation Maximization algorithm to compute the maximum likelihood estimator of the parameters, assuming a Gaussian distribution (mean 0 and variance σ^2) for the residuals (i.e., differences between predicted log viral load and measured log viral load) to quantify the error used in our simulations[51]. Individual parameters were subsequently computed using Markov Chain Monte Carlo (MCMC), and then best-fit estimates for each individual were calculated as Empirical Bayes Estimates (EBEs) (see Supplementary Note 1). The estimation procedures were performed using MONOLIX 2023R1 (www.lixoft.com).

Clustering algorithm to stratify mpox cases

We stratified the mpox cases using the K-means clustering algorithm[52], which finds cluster assignments by minimizing the sum of squared Euclidean distances between three estimated features: viral load at symptom onset, area under the viral load curve (AUC), and duration of viral shedding (see Supplementary Note 2). We first standardized the estimated features to ensure well-separated clusters, since they have different units. Then, the algorithm partitioned the set of estimated features into k clusters. The optimal number of clusters was determined by the Silhouette method[53]. To visualize the result of K-means clustering in a two-dimensional plane, we conducted a dimensionality reduction using principal component analysis (PCA)[54].

Simulation of viral dynamics and different rules for ending isolation

To account for individual variability in viral dynamics when determining the optimal duration of isolation, we simulated the predicted viral load, $V(t)$, for N virtual patients by running the viral clearance model. Parameter sets for each virtual patient were sampled from distributions of estimated model parameters. The measured viral load, $\hat{V}(t)$, was obtained from the following observation error model: $\log_{10} \hat{V}(t) = \log_{10} V(t) + \varepsilon, \varepsilon \sim N(0, \sigma^2)$, where ε is the error term. For each individual, the residuals were calculated at all measurement time points, and by fitting a Gaussian distribution to all computed residuals, the variance of error, σ^2, was estimated. Note that the variance for each virtual patient was assumed to be constant over time in the main analysis (i.e., constant error model). For parameter sets for virtual patients in each stratified group, we used individual parameters drawn from conditional distributions (i.e., distributions conditioned on the observed data and the estimated population parameters) characterizing the estimated parameters for individuals in each group, as estimated in the MCMC procedure. Additionally, as a sensitivity analysis, we considered a different observation error model whose variance is proportional to the predicted viral load (i.e., proportional error model): $\log_{10} \hat{V}(t) = \log_{10} V(t) + \varepsilon, \varepsilon \sim N(0, (\eta \log_{10} V(t))^2)$, where η is the proportional constant. The estimated parameter values in observation error models are summarized in Supplementary Table 3.

Under a symptom-based rule, as a current standard, patients would be released from isolation after the removal of lesions. For the timing of lesion clearance, maximum likelihood estimation (MLE) was used to fit parametric distributions to data on duration between symptom onset and lesion clearance for 43 mpox patients from the National Center for Global Health and Medicine (NCGM), Tokyo, Japan (see Supplementary Note 3). The timing of lesion removal for each patient was sampled from the best-fitted lognormal distribution (see Supplementary Fig. 3b and Supplementary Table 4). Additionally, as a sensitivity analysis, various relationships between individual viral dynamics and lesion clearance were considered. Specifically, we generated virtual mpox patient data under a range of possible values of the correlations between viral dynamics model parameters and the duration of lesion presence (see Supplementary Note 4). Under a fixed-duration rule, it was assumed that isolation would end at a specified time following symptom onset. On the other hand, under testing-based rules using tests, isolation ended when a given number of consecutive test results indicating loss of infectiousness was met with a given interval between tests. Here, we assumed that patients began to take tests immediately following symptom onset. To simulate various situations, we varied the interval between tests (from 1 to 5 days) and the number of consecutive test results indicating loss of infectiousness (from 1 to 5 times). To ascertain individuals' infectious periods, a viral load threshold of infectiousness was considered. If the viral load of a patient was above the threshold, the patient was considered as being infectious (see Supplementary Fig. 18). The threshold values considered were obtained from studies on viral replication in cell culture[23,32,33]. In this study, we set 6.0 log10 copies/ml as the main assumed infectiousness threshold value. However, this value is still uncertain and thus we also considered different threshold values from 5.0 to 7.0 log10 copies/ml as sensitivity analyses.

In particular, in the main analysis of testing-based rules, we considered PCR tests (limit of detection = 2.9 log10 copies/ml)[23], which can quantitatively measure viral load above the limit of detection to directly compare the measured viral load against the assumed infectiousness threshold. In this scenario, measured viral load can be used to determine whether an infected individual may no longer be infectious. Additionally, we considered rapid antigen tests (RATs) with lesion swabs, with either: 1) high sensitivity (i.e., limit of detection = 5.0 log10 copies/ml, lower than the assumed infectiousness threshold), or 2) low sensitivity (i.e., limit of detection = 7.0 log10 copies/ml, higher than the assumed infectiousness threshold). Under the testing-based rules using RATs, negative results correspond to a measured viral load below the limit of detection.

For the evaluation of different rules, three metrics were computed: (1) risk of prematurely ending isolation, (2) estimated infectious period after ending isolation, and (3) unnecessarily prolonged isolation period. The first metric gives the probability of releasing patients while they are still infectious. The second metric is defined as the mean number of days for which patients remain infectious after they are released from isolation (defined to be zero for an individual who is no longer infectious when released from isolation). The third metric gives the mean difference between the time when patients are no longer infectious and the time at which their isolation ends[9,10] (which is negative for individuals who are infectious beyond the end of isolation). Specifically, the risk of prematurely ending isolation was

computed as

$$\sum_{i=1}^{N} \frac{I(V_i(\tau_i) > IT)}{N}, \qquad (2)$$

where I is the indicator function, V_i is the predicted viral load of patient i, τ_i is the time when isolation of patient i ends, and IT is the assumed infectiousness threshold. Note that N stands for the number of virtual mpox patients and is set as 1000 in our analysis. We computed the infectious period after ending isolation by use of the following formula:

$$\sum_{i=1}^{N} \frac{\max(0, \bar{\tau}_i - \tau_i)}{N}, \qquad (3)$$

where $\bar{\tau}_i$ indicates the time when the predicted viral load of patient i drops below the assumed infectiousness threshold. Finally, the unnecessarily prolonged isolation period was calculated as

$$\sum_{i=1}^{N} \frac{(\tau_i - \bar{\tau}_i)}{N}. \qquad (4)$$

By running 100 simulations (N patients for each simulation), we reported the mean and 95% confidence intervals for distributions of those three metrics, respectively. All analyses were conducted using the statistical computing software R (version 4.2.3).

Reporting summary

Further information on research design is available in the Nature Portfolio Reporting Summary linked to this article.

Data availability

The mpox viral load data used in this study are publicly available and are also available via Zenodo[55]. Using WebPlotDigitizer-4.6, those data were extracted from the following publications: Suner et al. (https://doi.org/10.1016/S1473-3099(22)00794-0), Norz et al. (https://doi.org/10.1016/j.jcv.2022.105254), Adler et al. (https://doi.org/10.1016/j.jcv.2022.105254), Gaspari et al. (https://doi.org/10.1128/jcm.01365-22), Relhan et al. (https://doi.org/10.1002/jmv.28249), Hornuss et al. (https://doi.org/10.1016/j.cmi.2022.09.012), and Antinori et al. (https://doi.org/10.2807/1560-7917.ES.2022.27.22.2200421). The timing of lesion clearance data for mpox patients used in this study are publicly available. Those data were obtained from National Center for Global Health and Medicine (NCGM), Tokyo, Japan. Source data are provided with this paper.

Code availability

All analyses were performed with the statistical computing software R (version 4.2.3). The analysis using nonlinear mixed-effects model was performed on MONOLIX 2023R1 (www.lixoft.com). Our code is publicly available via Zenodo[55].

References

1. Vaughan, A. M. et al. A large multi-country outbreak of monkeypox across 41 countries in the WHO European Region, 7 March to 23 August 2022. *Euro Surveill.* **27**. https://doi.org/10.2807/1560-7917.ES.2022.27.36.2200620 (2022).
2. World Health Organization. 2022-23 Mpox Outbreak: global trends. https://worldhealthorg.shinyapps.io/mpx_global/ (2023).
3. Murayama, H. et al. Accumulation of immunity in heavy-tailed sexual contact networks shapes mpox outbreak sizes. *J. Infect. Dis.* https://doi.org/10.1093/infdis/jiad254 (2023).
4. Xiridou, M. et al. The fading of the mpox outbreak among men who have sex with men: a mathematical modelling study. *medRxiv*,
5. Brand, S. P. C. et al. The role of vaccination and public awareness in forecasts of Mpox incidence in the United Kingdom. *Nat. Commun.* **14**, 4100 (2023).
6. Endo, A., Jung, S. M. & Miura, F. Mpox emergence in Japan: ongoing risk of establishment in Asia. *Lancet* **401**, 1923–1924 (2023).
7. Thy, M. et al. Breakthrough Infections after Postexposure Vaccination against Mpox. *N. Engl. J. Med.* **387**, 2477–2479 (2022).
8. Raccagni, A. R. et al. Two individuals with potential monkeypox virus reinfection. *Lancet Infect. Dis.* **23**, 522–524 (2023).
9. Jeong, Y. D. et al. Revisiting the guidelines for ending isolation for COVID-19 patients. *Elife* **10**, e69340 (2021).
10. Jeong, Y. D. et al. Designing isolation guidelines for COVID-19 patients with rapid antigen tests. *Nat. Commun.* **13**, 4910 (2022).
11. Muller, J. & Kretzschmar, M. Contact tracing - old models and new challenges. *Infect. Dis. Model* **6**, 222–231 (2021).
12. Alpalhao, M. & Filipe, P. The impacts of isolation measures against SARS-CoV-2 infection on sexual health. *AIDS Behav.* **24**, 2258–2259 (2020).
13. Kretzschmar, M. E. et al. Impact of delays on effectiveness of contact tracing strategies for COVID-19: a modelling study. *Lancet Public Health* **5**, e452–e459 (2020).
14. Ash, T., Bento, A. M., Kaffine, D., Rao, A. & Bento, A. I. Disease-economy trade-offs under alternative epidemic control strategies. *Nat. Commun.* **13**, 3319 (2022).
15. Hossain, M. M., Sultana, A. & Purohit, N. Mental health outcomes of quarantine and isolation for infection prevention: a systematic umbrella review of the global evidence. *Epidemiol. Health* **42**, e2020038 (2020).
16. Leng, T., Hill, E. M., Keeling, M. J., Tildesley, M. J. & Thompson, R. N. The effect of notification window length on the epidemiological impact of COVID-19 contact tracing mobile applications. *Commun. Med.* **2**, 74 (2022).
17. Discontinuation of transmission-based precautions and disposition of patients with COVID-19 in healthcare settings (interim guidance). https://stacks.cdc.gov/view/cdc/88538 (2020).
18. Infection prevention and control of mpox in healthcare settings. https://www.cdc.gov/poxvirus/mpox/clinicians/infection-control-healthcare.html (2022).
19. Centers for Disease Control and Prevention (CDC). Considerations for reducing mpox transmission in congregate living settings, https://www.cdc.gov/poxvirus/mpox/community/congregate.html (2022).
20. Maya, S. & Kahn, J. G. COVID-19 testing protocols to guide duration of isolation: a cost-effectiveness analysis. *BMC Public Health* **23**, 864 (2023).
21. Miura, F. et al. Time scales of human mpox transmission in the Netherlands. *J. Infect. Dis.* https://doi.org/10.1093/infdis/jiad091 (2023).
22. Madewell, Z. J. et al. Serial interval and incubation period estimates of monkeypox virus infection in 12 jurisdictions, United States, May-August 2022. *Emerg. Infect. Dis.* **29**, 818–821 (2023).
23. Suner, C. et al. Viral dynamics in patients with monkeypox infection: a prospective cohort study in Spain. *Lancet Infect. Dis.* **23**, 445–453 (2023).
24. Gaspari, V. et al. Monkeypox Outbreak 2022: clinical and virological features of 30 patients at the sexually transmitted diseases centre of Sant' Orsola Hospital, Bologna, Northeastern Italy. *J. Clin. Microbiol.* **61**, e0136522 (2023).
25. European Centre for Disease Prevention and Control. Factsheet for health professionals on mpox (monkeypox). https://www.ecdc.europa.eu/en/all-topics-z/monkeypox/factsheet-health-professionals (2023).

2023.2001.2031.23285294. https://doi.org/10.1101/2023.01.31.23285294 (2023).

26. Centers for Disease Control and Prevention (CDC). Isolation and prevention practices for people with mpox. https://www.cdc.gov/poxvirus/mpox/clinicians/isolation-procedures.html (2023).

27. UK Health Security Agency. Mpox (monkeypox): people who are isolating at home. https://www.gov.uk/guidance/guidance-for-people-with-monkeypox-infection-who-are-isolating-at-home (2022).

28. National Institute for Public Health and the Environment. Information letter for a person with monkeypox. https://lci.rivm.nl/information-letter-person-monkeypox (2022).

29. Adler, H. et al. Clinical features and management of human monkeypox: a retrospective observational study in the UK. *Lancet Infect. Dis.* **22**, 1153–1162 (2022).

30. Jones, B. et al. Variability in clinical assessment of clade IIb mpox lesions. *Int. J. Infect. Dis.* **137**, 60–62 (2023).

31. Luciani, L. et al. A novel and sensitive real-time PCR system for universal detection of poxviruses. *Sci. Rep.* **11**, 1798 (2021).

32. Saijo, M. et al. Diagnosis and assessment of monkeypox virus (MPXV) infection by quantitative PCR assay: differentiation of Congo Basin and West African MPXV strains. *Jpn. J. Infect. Dis.* **61**, 140–142 (2008).

33. Norz, D. et al. Evidence of surface contamination in hospital rooms occupied by patients infected with monkeypox, Germany, June 2022. *Euro Surveill.* **27**, 2200477 (2022).

34. Kapmaz, M. et al. A complicated case of monkeypox and viral shedding characteristics. *J. Infect.* **86**, 66–117 (2023).

35. White, J. A., et al. Complex decay dynamics of HIV virions, intact and defective proviruses, and 2LTR circles following initiation of anti-retroviral therapy. *Proc. Natl Acad. Sci. USA* **119** (2022).

36. Endo, A. et al. Heavy-tailed sexual contact networks and monkeypox epidemiology in the global outbreak, 2022. *Science* **378**, 90–94 (2022).

37. Thompson, R. N. et al. Improved inference of time-varying reproduction numbers during infectious disease outbreaks. *Epidemics* **29**, 100356 (2019).

38. De Baetselier, I. et al. Retrospective detection of asymptomatic monkeypox virus infections among male sexual health clinic attendees in Belgium. *Nat. Med.* **28**, 2288–2292 (2022).

39. Ejima, K. et al. Estimation of the incubation period of COVID-19 using viral load data. *Epidemics* **35**, 100454 (2021).

40. Chen, P. Z. et al. SARS-CoV-2 shedding dynamics across the respiratory tract, sex, and disease severity for adult and pediatric COVID-19. *Elife* **10**. https://doi.org/10.7554/eLife.70458 (2021).

41. Tronstein, E. et al. Genital shedding of herpes simplex virus among symptomatic and asymptomatic persons with HSV-2 infection. *JAMA* **305**, 1441–1449 (2011).

42. Mouliou, D. S. & Gourgoulianis, K. I. False-positive and false-negative COVID-19 cases: respiratory prevention and management strategies, vaccination, and further perspectives. *Expert Rev. Respir. Med.* **15**, 993–1002 (2021).

43. Norz, D. et al. Clinical characteristics and comparison of longitudinal qPCR results from different specimen types in a cohort of ambulatory and hospitalized patients infected with monkeypox virus. *J. Clin. Virol.* **155**, 105254 (2022).

44. Relhan, V. et al. Clinical presentation, viral kinetics, and management of human monkeypox cases from New Delhi, India 2022. *J. Med Virol.* **95**, e28249 (2023).

45. Hornuss, D. et al. Transmission characteristics, replication patterns and clinical manifestations of human monkeypox virus-an in-depth analysis of four cases from Germany. *Clin. Microbiol Infect.* **29**, 112 e115–112 e119 (2023).

46. Antinori, A. et al. Epidemiological, clinical and virological characteristics of four cases of monkeypox support transmission through sexual contact, Italy, May 2022. *Euro Surveill.* **27**. https://doi.org/10.2807/1560-7917.ES.2022.27.22.2200421 (2022)

47. Ministry of Health, Labour and Welfare, Japan. Mpox treatment guideline. https://www.mhlw.go.jp/content/001183682.pdf (2023).

48. Centers for Disease Control and Prevention (CDC). Mpox. Guidance for tecovirimat use. https://www.cdc.gov/poxvirus/mpox/clinicians/Tecovirimat.html (2023).

49. Palich, R. et al. Viral loads in clinical samples of men with monkeypox virus infection: a French case series. *Lancet Infect. Dis.* **23**, 74–80 (2023).

50. Kim, H. et al. Viral load dynamics and shedding kinetics of mpox infection: a systematic review and meta-analysis. *J. Travel Med.* **30**. https://doi.org/10.1093/jtm/taad111 (2023).

51. Kuhn, E. & Lavielle, M. Maximum likelihood estimation in nonlinear mixed effects models. *Comput. Stat. Data Anal.* **49**, 1020–1038 (2005).

52. Sammut, C. & Webb, G. I. *Encyclopedia of Machine Learning* (Springer Science & Business Media, 2011).

53. Rousseeuw, P. J. & Kaufman, L. *Finding Groups in Data: an Introduction to Cluster Analysis* (John Wiley & Sons Hoboken, New Jersey, 2009).

54. Jolliffe, I. T. & Cadima, J. Principal component analysis: a review and recent developments. *Philos. Trans. A Math. Phys. Eng. Sci.* **374**, 20150202 (2016).

55. Jeong, Y. D. Modelling the effectiveness of an isolation strategy for managing mpox outbreaks with variable infectiousness profiles. https://doi.org/10.5281/zenodo.12561102 (2024).

Author contributions
S.I. and F.M. designed the research. Y.D.J., W.S.H., and R.N.T. carried out the computational analysis. S.I., R.N.T., M.I., and F.M. supervised the project. Y.D.J., W.S.H., R.N.T., M.I., T.N., H.P., N.I., A.S., M.S., K.A., K.W., E.O.d.C., N.O., J.W., S.I., and F.M. wrote the paper. All authors discussed the research and approved the final manuscript.

Competing interests
The authors declare no competing interests.

Additional information

[1]Interdisciplinary Biology Laboratory (iBLab), Division of Natural Science, Graduate School of Science, Nagoya University, Nagoya, Japan. [2]Department of Mathematics, Pusan National University, Busan 46241, South Korea. [3]Mathematical Institute, University of Oxford, Oxford OX2 6GG, UK. [4]Disease Control and Prevention Centre, National Centre for Global Health and Medicine, Tokyo, Japan. [5]International Research Center for Neurointelligence, The University of Tokyo Institutes for Advanced Study, The University of Tokyo, Tokyo, Japan. [6]Research Center for Drug and Vaccine Development, National Institute of Infectious Diseases, Tokyo, Japan. [7]Centre for Infectious Disease Control, National Institute for Public Health and the Environment (RIVM), Bilthoven, The Netherlands. [8]Department of Biomedical Data Sciences, Leiden University Medical Center (LUMC), Leiden, The Netherlands. [9]Institute of Mathematics for Industry, Kyushu University, Fukuoka, Japan. [10]Institute for the Advanced Study of Human Biology (ASHBi), Kyoto University, Kyoto, Japan. [11]Interdisciplinary Theoretical and Mathematical Sciences Program (iTHEMS), RIKEN, Saitama, Japan. [12]NEXT-Ganken Program, Japanese Foundation for Cancer Research (JFCR), Tokyo, Japan. [13]Science Groove Inc., Fukuoka, Japan. [14]Center for Marine Environmental Studies (CMES), Ehime University, Matsuyama, Ehime, Japan. [15]These authors contributed equally: William S. Hart, Robin N. Thompson, Masahiro Ishikane. [16]These authors jointly supervised this work: Shingo Iwami, Fuminari Miura. ✉e-mail: iwami.iblab@bio.nagoya-u.ac.jp; fuminari.miura@rivm.nl